

OBSERVATIONS ON SPATIAL RELATIONSHIPS OF IMPACT CRATER FLOOR MORPHOLOGIES IN THE SINUS SABAEUS REGION OF MARS. N. K. Forsberg-Taylor¹ and A. D. Howard¹, ¹Department of Environmental Sciences, University of Virginia, Charlottesville, VA 22903 (nforsberg@virginia.edu)

Introduction: Impact cratering is arguably the most important surficial geologic process occurring on the terrestrial planets (with the exception of Earth). Since impact craters can be considered closed systems, they are excellent tools for measuring the degree and type of erosion occurring on a planet's surface.

Until recently, studying the geomorphic features of impact craters on Mars has been difficult due to poor data resolution. However, within the last decade, the Mars Orbiter Laser Altimeter (MOLA) has returned high resolution topographic data of the Martian surface. Using these data and images of Mars returned from the Viking missions, we have created a comprehensive database of degradational characteristics of the craters in the Sinus Sabaeus region of Mars. The purpose of this study is to gain a better understanding of the past and present surface processes that modify the surface topography of Mars.

Site Description: The Sinus Sabaeus region of Mars covers an area approximately bounded by 0N and 30S latitude, and 315W and 360W longitude. Located in the southern highlands, this area is heavily cratered and Noachian in age [1]. Sinus Sabaeus is topographically fairly homogenous. Thermal inertia measurements of the area indicate that the surface is covered by a thick layer of sand-sized to fine-grained sediments, inferred to be the result of eolian deposition. Mars Orbiter Camera (MOC) images have shown that the layer of sediment varies in thickness from location to location in the region. The rock abundance of the region has been estimated to be less than or equal to 10% [2,3,4].

Data Sets and Methods: In this study, we have used both imagery and topographic data to collect information about the craters. The images of Mars were collected by the Viking Orbiter missions (MDIMs) and have a resolution of at least 400m/pixel. Each covers an area of approximately 5 degrees latitude by 5 degrees longitude. The second dataset used consists of topographic data collected by MOLA and has a nominal vertical resolution of approximately 0.5m and a horizontal resolution of approximately 330 m [5]. The resolution of this data is approximately 1 km², although the spacing between the tracks was essentially random, so some gaps of several kilometers between tracks have occurred.

Craters larger than 10 km in diameter were chosen for this study due to the resolution limitations of the MOLA data. Each crater was studied both qualitatively

and quantitatively. Using the MDIMs, crater degradation levels were estimated visually using a classification scheme developed in Craddock, et al. [6]. Degradation classes ranged from Type A, referring to very fresh craters (with central peaks, sharp rims and ejecta blankets), to Type E, referring to the most degraded craters (with no rim and an irregular floor). For each crater chosen for study, a topographic map was created using the MOLA data. From this map, the crater's geometric center, lowest elevation region and rim boundaries were located using the program Surfer (Figure 1). This information was then inputted into a FORTRAN program that accessed all of the raw topographic data for the crater out to a distance of two crater diameters from the center. Within the FORTRAN program, each crater was divided into eight equal 45-degree sectors. Information was averaged within each sector. This information was used to calculate values such as average depth, rim diameter, rim height, floor diameter and maximum wall slope of the crater.

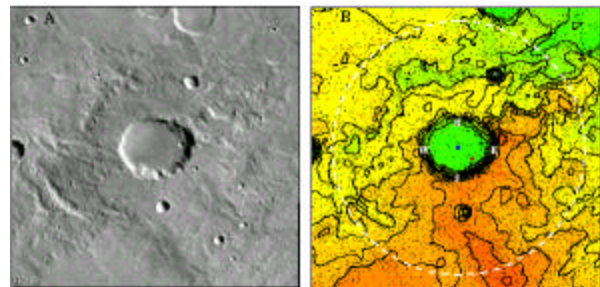
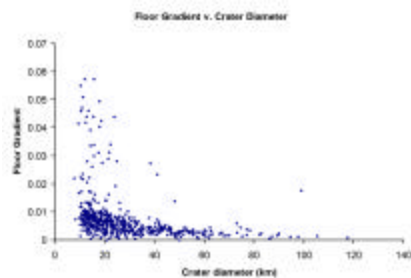


Figure 1. Example of data collection for each crater. **A** is an MDIM of an approximately 13-km diameter crater. **B** is the corresponding DEM created with Surfer using MOLA data. *N,S,W,E* represent the points used to determine the crater's diameter and geometric center. \downarrow represents the geometric center of the crater. $?$ represents the low point center of the crater. The white dashed line represents the 2-crater diameter boundary of the study area for this crater.

Results and Observations: Approximately 700 craters with diameters greater than 10 km and with sufficient MOLA coverage are present in the Sinus Sabaeus region. There are approximately 200 other craters in the region that do fall within the size restrictions but do not have complete MOLA coverage and are therefore being used only in gross regional calculations, such as relative age dating.

Many different morphologic features of the impact craters are being studied. One such feature that we are focusing on presently is the crater floor. We are defining the floor as the region enclosed by the points of minimum curvature along the crater profile, or where the slope of the profile increases drastically, marking the point where the flatter floor meets the steep wall.

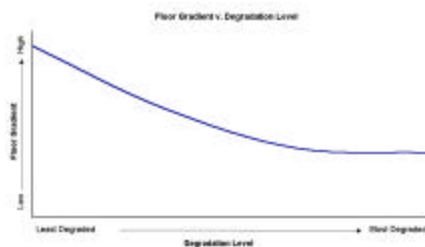
Floor gradient: Using the raw topography data and the averaged profiles returned from the FORTRAN program, we were able to calculate the gradient of the crater floors. The gradient was calculated as the elevation change from the geometric center of the crater (ignoring central peaks when present) to the point of minimum curvature (the floor/wall boundary) over the radius of the crater floor. It has been revealed that as the diameter of the crater increases, the floor gradient decreases significantly, with few small craters possessing highly sloped floors. These are interpreted to be the freshest craters in the region [Graph 1].



Graph 1. Floor gradient vs crater diameter for the region. Note: gradient tends to decrease as diameter increases.

When floor gradients are compared to the initial degradation classes assigned to the craters, the average slope decreases from 0.015 for the fresh craters to 0.006 for the most highly degraded craters. The floor gradient varies according to the curve in Graph 2.

Graph 2. Change in floor gradient with change in degradation level seen in the craters of the region.



Floor smoothness: Cross-sectional profiles were created for each crater. These profiles were visually classified based on floor smoothness as 'smooth floored,' 'relatively smooth floored' or 'other' [Figure 2]. In the smooth floored craters, all of the cross-sectional profiles match and there are no significant elevation changes along the crater floor. Relatively smooth floored crater profiles are relatively consistent, but there is some variation in elevation along the floor.

'Other' craters have inconsistent profiles and significant elevation variation along the crater floor.

When the spatial locations of these three visual classifications are plotted, it is revealed that the smooth and relatively smooth floored craters occur predominantly in the eastern portion of the region [Figure 3]. This area is higher in elevation and less degraded overall than the western portion of the region. The majority of the craters with the smoother floors appear to be relatively fresh, inasmuch as they possess intact rims. It can be hypothesized that the floor smoothness is the result of a relative short-term, distinct process that worked to create a smooth crater floor without eroding the crater rim.

As future work, we will use the topographical data to quantitatively calculate the floor smoothness.

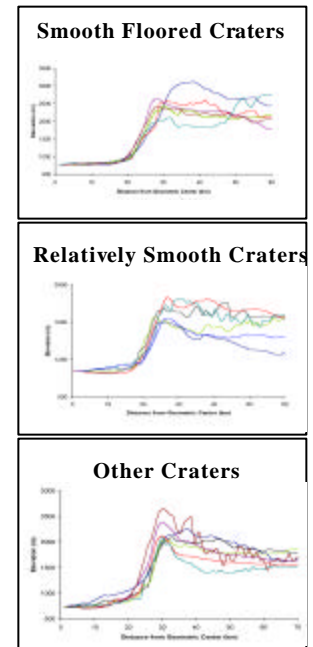


Figure 2. Examples of the three visual classifications of crater floor smoothness.

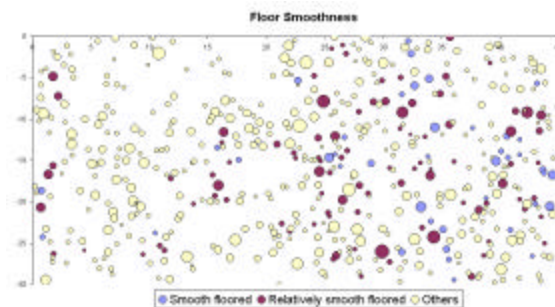


Figure 3. Locations of the different floor smoothnesses present in the region. Note that smoother floored craters occur predominantly in the eastern portion.

References: [1] Tanaka K. L., et al. (1992) in *Mars* (H.H. Keiffer, et al., eds.) [2] Edgett, K. S. and Malin, M. C. (2000) *JGR*, 105, 1,623-1,650. [3] Malin, M. C. and Edgett, K. S. (2001) *JGR*, 106 23,429-23,570. [4] Edgett, K. S. and Christensen, P. R. (1991) *JGR*, 96, 22,765-22,776. [5] Garvin, J. B. and Frawley, J. J. (1998) *GRL*, 25, 4,405-4,408. [6] Craddock, R. A., et al. (1997) *JGR*, 102, 13,321-13,340.